GA A27342

DISRUPTION RUNAWAY ELECTRON DISSIPATION AND ENERGY DISTRIBUTION IN DIII-D

by

E.M. HOLLMANN,* J.A. BOEDO,* N.H. BROOKS, N. COMMAUX, N.W. EIDIETIS, T.E. EVANS, D.A. HUMPHREYS, V.A. IZZO,* T.C. JERNIGAN, R.A. MOYER,* J.M. MUÑOZ-BURGOS, P.B. PARKS, D.L. RUDAKOV,* E.J. STRAIT, C. TSUI,¶ M.A. VAN ZEELAND, J.C. WESLEY, and J.H. YU*

This is a preprint of a paper to be presented at the Thirty-ninth European Physical Society Conf., on Plasma Physics, July 2 6, 2012 in Stockholm, Sweden and to be published in the Proceedings.

*University of California San Diego, La Jolla, California, USA.
Oak Ridge National Laboratory, Oak Ridge, Tennessee, USA.
Oak Ridge Institute for Science Education, Oak Ridge, Tennessee, USA.

Work supported in part by
the U.S. Department of Energy under
DE-FG02-07ER54917, DE-FC02-04ER54698, DE-FG02-95ER54309,
DE-AC05-00OR22725, and DE-AC05-06OR23100

GENERAL ATOMICS PROJECT 30200
JUNE 2012

Disruption Runaway Electron Dissipation and Energy Distribution in DIII-D

E.M. Hollmann[1], J.A. Boedo[1], N.H. Brooks[2], N. Commaux[3], N.W. Eidietis[2], T.E. Evans[2], D.A. Humphreys[2], V.A. Izzo[1], T.C. Jernigan[3], R.A. Moyer[1], J.M. Muñoz-Burgos[4], P.B. Parks[2], D.L. Rudakov[1], E.J. Strait[2], C. Tsui[5], M.A. Van Zeeland[2], J.C. Wesley[2], and J.H. Yu[1]

[1]*University of California San Diego, La Jolla, California 92093-0417, USA*
[2]*General Atomics, PO Box 85608, San Diego, California 92186-5608, USA*
[3]*Oak Ridge National Laboratory, PO Box 2008, Oak Ridge, Tennessee 37831, USA*
[4]*Oak Ridge Institute for Science Education, Oak Ridge, Tennessee 37830-8050, USA*
[5]*University of Toronto Institute for Aerospace Studies, Toronto M3H 5T6, Canada*

Understanding the structure and dynamics of runaway electron (RE) beams formed at the end of tokamak disruptions is important for understanding how to control and dissipate these REs and to predict to the damage REs can do to tokamak walls. In DIII-D, high current (0.1–0.5 MA) RE beams are created by rapidly terminating discharges with small (2.7 mm) argon pellet injection. Control system changes have been implemented that allow the RE beam to be held centered, avoiding the rapid (~1 ms) loss of the REs that occurs when the plasma radius falls below 0.3 m and contacts the inner wall [1]. Even when not contacting the wall, the RE current decays with time. Comparisons of the measured RE current decay with avalanche theory indicate that there is an anomalous high decay $\left(dI_p/dt\right)/I_p \approx -10/\text{s}$ [2]. This assumes a top-hat RE beam profile with no neutral penetration into the RE channel. Here, improved data analysis is presented which supports these assumptions. Also, data is presented that suggests the anomalous RE current decay is due to the presence of argon ions in the RE beam.

The data used here is line-integrated through the plasma, so inversions are necessary to estimate radial variations of electron and atom densities. Two types of inversions are used here: (a) inversions of soft x-ray (SXR) and interferometer data are performed on fast, downward-scanning plasmas to demonstrate that both hot and cold electron densities are reasonably approximated by magnetic flux contours; and (b) inversions of line-integrated spectrometer data are done on stationary plasmas in order to demonstrate that neutrals are excluded from the hot plasma core. The fast, downward scanning inversions only assume that magnetic reconstructions are correctly capturing the relative motion of the center of the plasma and that the plasma shape remains fixed relative to the center during the downward motion. The stationary inversions then assume that plasma emissivity contours follow magnetic surface contours.

Inversions of downward-scanning plasmas are shown in Fig. 1. The total electron density consists of two components: a cold, dense background plasma ($T_e \approx 1.5$ eV, $n_e \approx 10^{14}$ cm^{-3}) and a hot, tenuous RE beam component (energy ~ several MeV, $n_e \approx 10^{10}$ cm^{-3}). The line-integrated cold background plasma electron density can be measured with interferometers and the line-integrated hot electron density can be estimated from SXR view chords. Figure 1(a) shows SXR view chords and magnetic flux surface reconstructions during

downward motion. The flux surfaces are calculated with a current filament inversion code (JFIT) constrained with external magnetic sensors. Figure 1(b) shows measured SXR brightness vs channel number for three different time steps, as well as back-constructed SXR brightness from the inversion, showing a reasonably good fit. Figure 1(c) shows SXR emissivity contours and JFIT contours. Typically, we find that the SXR center and the JFIT center are within 10 cm of each other, with no clear systematic shift. Figure 1(d–f) shows the reconstructed cold electron density profile; it can be seen that the cold electron profile 1(f) is much broader than the hot electron density profile 1(c).

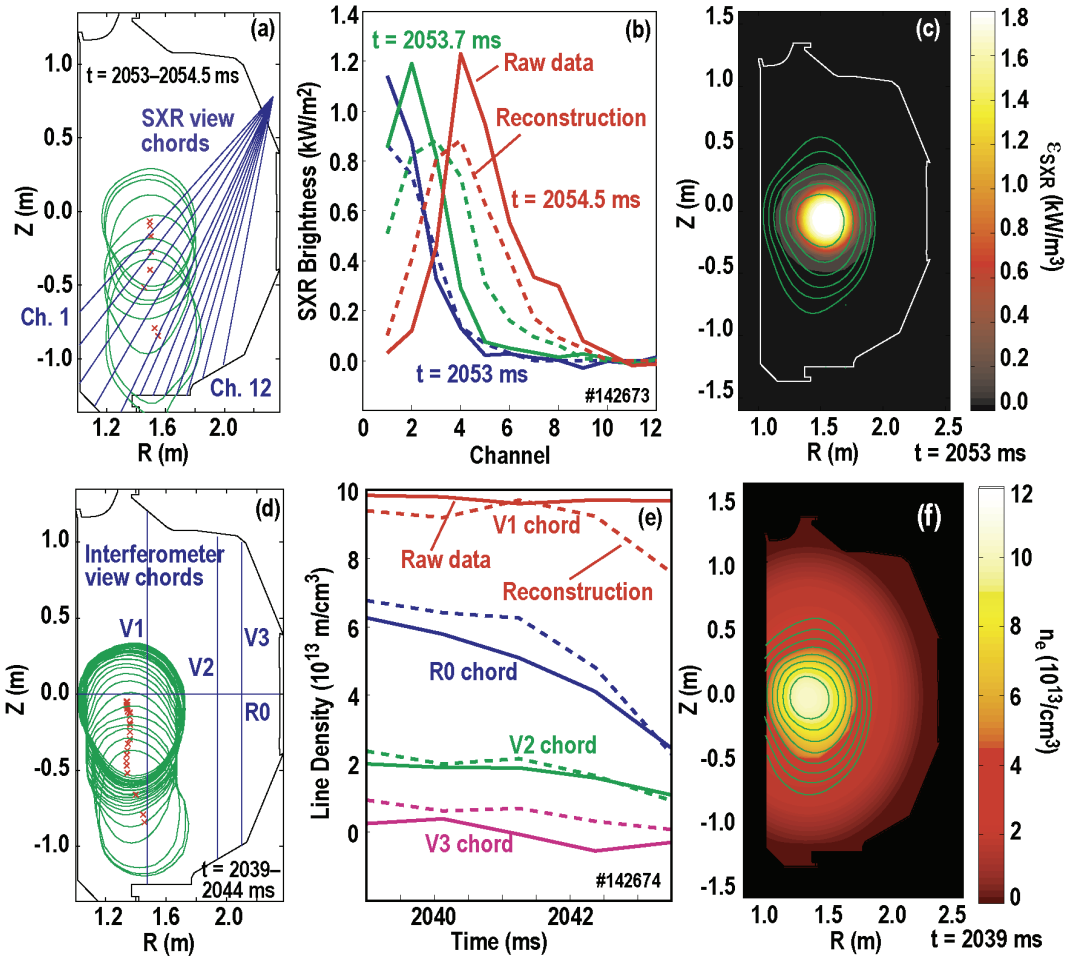

Fig. 1. SXR inversion showing: (a) JFIT reconstructions of flux surfaces of downward moving RE beam (beam is higher at early times), (b) SXR brightness vs array channel number at different time steps, and (c) reconstructed SXR emissivity and JFIT flux surfaces; interferometer inversion showing: (d) JFIT reconstructions of flux surfaces, (e) line-integrated data vs time, and (f) reconstructed cold electron density contours.

Tangential visible camera images suggest that visible line emissivity is a reasonably good flux function [2]. Using JFIT contours as line emissivity contours, it is then possible to use line-integrated visible line brightness data from stationary RE plateau plasmas to make estimates of the ion and neutral densities in the RE beam. Deuterium density can be estimated from D_α (656.2 nm) brightness, Ar^+ density from Ar-II (465.8 nm) brightness, Ar density from Ar-I (811.5 nm) brightness, and C^+ density from C-II (657.8 nm) brightness. Upward-viewing poloidal view fans are used for Ar-I, Ar-II, and D_α; while a tangential fan is used for C-II brightness. Photon emission coefficients from ADAS [3] are used. The D^+ density can

then be estimated from quasi-neutrality using the interferometer data. Figure 2 shows the resulting profiles for (a) D and D^+ and (b) Ar and Ar^+. The quality of the reconstructed line-integrated data is shown in panes (c) for interferometer data, (d) for Ar-I brightness, (e) for Ar-II brightness, and (f) for D_α brightness. Overall, it can be seen that the data is fit within a factor of two or better across the plasma profile. Neutrals are seen to be mostly excluded from the RE beam core of radius 0.3 m. C^+ density, not shown here, is found to be small (~1%) in the RE beam core. Argon ion content is found to be about 5% in the RE beam core. Compared with the initial amount of argon in the injected pellet (2.3×10^{20} argon atoms), only 5% of the injected argon appears accounted for in the RE beam. The bulk of the argon apparently remains as neutrals outside the RE beam.

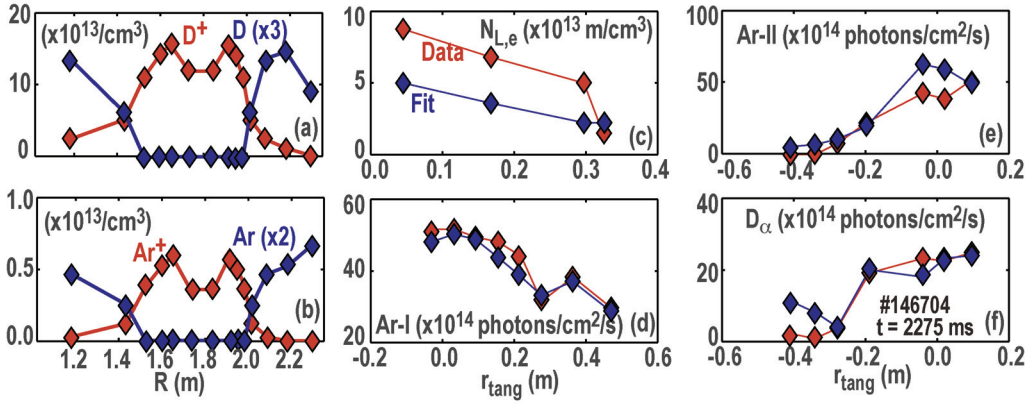

Fig. 2. Midplane density profiles at t = 2275 ms for (a) deuterium neutrals and ions and (b) argon neutrals and ions as a function of midplane radius. (c–f) show quality of fits to line-integrated electron density and line brightnesses. r_{tang} is distance of closest approach of view chord to magnetic axis, with negative values indicating view chord passes between magnetic axis and center post.

For the fits shown in Fig. 2(c–f), the radial electron temperature profile was varied as a free parameter. A central electron temperature of about 1.5 eV and edge temperature of about 0.8 eV are obtained. These are roughly consistent with measured line widths of about 1.6 eV for ions and 1.2 eV for neutrals. This suggests that the visible line emission is dominated by cold electrons collisions, not hot electron collisions.

Using the observation that neutrals appear to be excluded from the hot core, the ion density in the RE beam can be estimated in shots where massive gas injection (MGI) is fired into the RE beam by assuming that the added electron density is entirely due to singly-charged ions (e.g. electron density rise following neon MGI is due entirely to Ne^+ ions). Multiply-charged ions are thought to be negligible, as they are barely observable in visible or UV spectrometers. Given an ion density and electron density, a free and bound electron density can be obtained, and the expected RE current dissipation rate due to standard avalanche theory (electron-electron collisions) calculated [4].

Figure 3(a) shows measured and expected RE current decay rates $(dI_p/dt)/I_p$ for several shots. It can be seen that the standard condition (Ar pellet only) has a discrepancy between theory and measurement of $(dI_p/dt)/I_p \approx$ -10/s. In shots where additional high-Z ions are added (from neon or argon MGI), the magnitude of the discrepancy is even larger, $(dI_p/dt)/I_p \approx$ -20/s. In shots where low-Z ions (deuterium or helium) are added, the magnitude of the

discrepancy becomes smaller, down to $(dI_p/dt)/I_p$ < -5/s. These results indicate that the anomalous dissipation may be due to the presence of high-Z ions in the plasma, possibly due to pitch angle scattering. Pitch angle scattering of fast electrons could reduce RE current directly, by collisional drag on the RE distribution, or indirectly, by causing enhanced loss of REs to the wall. Evidence for both possibilities exist. RE loss to the wall is seen in SXR chords when the RE beam is moved very close to the wall (within 0.3 m) so some slow diffusive loss is presumably occurring even when the RE beam is farther from the wall, although this has not been quantified yet.

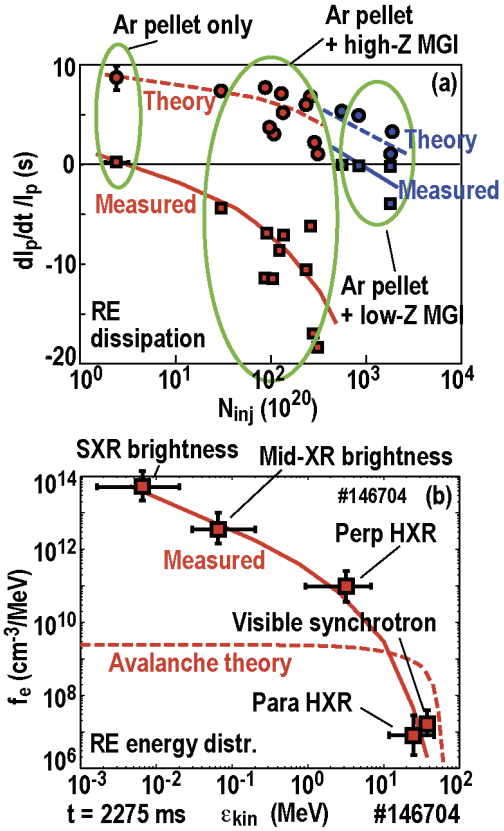

Fig. 3. (a) RE current decay rate as a function of the number of injected particles and (b) RE energy distribution function measured for baseline case (Ar pellet injection only).

Evidence for anomalous drag on the RE distribution is seen in the measured distribution function, Fig. 3(b). This is assembled from different diagnostics, each dominantly sensitive to a different part of the RE energy distribution: SXR detectors (mostly sensitive to electrons in the 2–20 keV range), CdTe mid x-ray detectors (mostly sensitive to electrons in the 20–200 keV range), perpendicular-viewing BGO hard x-ray (HXR) detectors (mostly sensitive to electrons in the 1–5 MeV range), parallel-viewing HXR detectors (mostly sensitive to electrons in the 10–50 MeV range), and visible synchrotron emission (mostly sensitive to electrons in the 30–50 MeV range). X-ray brightnesses are calculated using the bremsstrahlung simulations of Ref. [5] parametrized analytically as done in the GEANT4 code. The dashed line is the distribution function expected from avalanche theory, $f_{RE}(p) \sim exp(-p/m_e c\bar{p})$, with $p \equiv m_e c\beta\gamma$ and $\bar{p} \equiv [3(Z+5)/\pi]^{1/2} ln[\Lambda(Z)] \approx 46$ for argon [6]; the normalization is obtained from the plasma current, assuming all plasma current is carried by the fast electrons. It can be seen that the measured distribution function appears skewed toward low energies, possibly indicating an anomalous collisional drag on the fast electrons. Future work will attempt to isolate whether the observed anomalous RE loss comes from drag on the REs or loss of REs to the plasma wall.

This work was supported in part by the US Department of Energy under DE-FG02-07ER54917, DE-FC02-04ER54698, DE-AC05-00OR22725, and DE-AC05-06OR23100.

[1] N.W. Eidietis, *et al.*, Phys. Plasmas **19** (2012) 056109.
[2] E.M. Hollmann, *et al.*, Nucl. Fusion **51** (2011) 103026.
[3] H.P. Sommers, *et al.*, Plasma Phys. Controlled Fusion **44** (2002) B323.
[4] M.N. Rosenbluth and S.V. Putvinski, Nucl. Fusion **37** (1997) 1355.
[5] S.M. Seltzer and M.J. Berger, Nucl. Instrum. Methods **12** (1985) 95.
[6] P.B. Parks, M.N. Rosenbluth, and S.V. Putvinski, Phys. Plasmas **6** (1999) 2523.